electronics

MDPI

Article

LSTM-Based MPPT Algorithm for Efficient Energy Harvesting of a Solar PV System Under Different Operating Conditions

Anushka Bandara [1], Keshawa Ratnayake [1], Ramitha Dissanayake [1], Harith Udawatte [1], Roshan Godaliyadda [1], Parakrama Ekanayake [1] and Janaka Ekanayake [1,2,*]

[1] Department of Electrical and Electronic Engineering, University of Peradeniya, Peradeniya 20400, Sri Lanka; anushkab@ee.pdn.ac.lk (A.B.); keshawar@eng.pdn.ac.lk (K.R.); e15084@eng.pdn.ac.lk (R.D.); harith.udawatte@eng.pdn.ac.lk (H.U.); roshang@eng.pdn.ac.lk (R.G.); mpbe@eng.pdn.ac.lk (P.E.)
[2] Center for Integrated Renewable Energy Generation and Supply, Cardiff University, Cardiff CF10 3AT, UK
* Correspondence: ekanayakej@cardiff.ac.uk; Tel.: +94-777146979

Abstract: Solar energy is one of the most favorable renewable energy sources and has undergone significant development in the past few years. This paper investigates a novel concept of harvesting the maximum power of a photovoltaic (PV) system using a long-short term memory (LSTM) to forecast the irradiance value and a feedforward neural network (FNN) to predict the maximum power point (MPP) voltage. This study paves a way to mitigate avoidable inefficiencies that hinder the optimal performance of a PV system, due to the intermittent nature of solar energy. MATLAB/Simulink software platform was used to validate the proposed algorithm with real irradiance data from different geographical and weather conditions. Furthermore, the maximum power point tracking (MPPT) algorithm was implemented in a laboratory setup. The simulation results portray the superiority of the proposed method in terms of tracking performance and dynamic response through a comprehensive case study conducted with five other state-of-the-art MPPT methods selected from conventional, AI based, and bio-inspired MPPT categories. In addition to that, faster response time and lesser oscillations around the MPP were observed, even during volatile weather conditions and partial shading.

Keywords: renewable energy; maximum power point tracking; long-short term memory; partial shading

check for updates

Citation: Bandara, A.; Ratnayake, K.; Dissanayake, R.; Udawatte, H.; Godaliyadda, R.; Ekanayake, P.; Ekanayake, J. LSTM-Based MPPT Algorithm for Efficient Energy Harvesting of a Solar PV System Under Different Operating Conditions. *Electronics* **2024**, *13*, 4875. https://doi.org/10.3390/electronics13244875

Academic Editor: Dorin Petreus

Received: 6 November 2024
Revised: 7 December 2024
Accepted: 8 December 2024
Published: 11 December 2024

1. Introduction

Renewable energy has shown exponential growth over the past decade in the energy production sector along with research developments that enhanced its efficiency and reliability in enervating from sources such as solar and wind. When considering these renewables, solar energy has played a pivotal role and is regarded as the most promising alternative to fossil fuels mainly due to its cleanliness, abundance, and environmental friendliness [1,2]. However, photovoltaic (PV) systems face challenges due to their unpredictability, primarily caused by fluctuating weather conditions. The efficiency of a PV system is affected by numerous factors such as inverter conversion losses, thermal losses, and failure to track the maximum power point (MPP). Out of these, 5–30% efficiency reduction may occur due to the failure of converging to the MPP. When the installed capacity is high, this loss is substantial [3]. Therefore, it is essential to adapt maximum power point tracking (MPPT) techniques to ensure that the highest possible power is harvested from a PV array under different operating conditions.

Extensive research on MPPT methods has been undertaken, and hence various techniques that differ according to aspects such as tracking mechanism, implementations, and modernity [4] can be found in the literature. Generally, these methods can be classified into conventional, soft-computing, and hybrid. Perturb and Observe (P&O) [5–7], incremental conductance (InC) [6–10], hill climbing, and constant voltage (CV) [4] are some popular conventional methods. The main advantages of these methods are their simplicity and easy implementation. However, these conventional methods suffer from low tracking speed, low efficiency, and high oscillations around the MPP. Thus, various developments have been introduced to mitigate these limitations of conventional methods [11,12]. To overcome the aforementioned limitations, soft computing-based methods have been introduced which can be identified as artificial intelligence (AI)-based methods and bio-inspired methods [13]. Despite their complex nature and considerable cost to implement, these methods depict satisfactory performance in partial shading (PS) conditions due to their robustness, flexibility, and reliability [4]. Widely used AI-based methods are the artificial neural network (ANN) [2,3] and fuzzy-logic control (FLC) [2,7,8], while the particle swarm optimization (PSO) and genetic algorithm are the two most common bio-inspired methods [2,4,7] found in the literature. ANNs are computational models inspired by the human brain and typically a feed-forward architecture with three layers is used. On the other hand, the most critical aspect of FLCs is converting inaccurate and qualitative information into numerical values. Importantly, these methods are favorable in practical conditions where uncertainties exist, such as unpredictable changes, nonlinearity, and unmodeled quantities. However, heuristic methods like PSO show high potential due to their simple structure, easy implementation, and fast computation capability [7,14]. PSO is considered the best method to work under partial shading conditions mostly because of its high ability to find a global maximum power point (GMPP) [4]. On the contrary, the computational burden is comparatively larger than that of the conventional methods, and these methods also display significant oscillations and consume more time as they undergo a large random search [15].

Recently, hybrid MPPT methods, which typically combine two conventional methods, one conventional method and one soft computing method, or two soft computing methods, have become popular. These are developed to perform mutual cancellation [16] of open issues and provide high and robust performance in tracking the maximum power point. To obtain a high-power efficiency and fast response, the P&O method and CV method are fused in [17] and both simulation and experimental results have proven the novel algorithm's superior performance to other state-of-the-art methods. In [18], the authors propose a hybrid method which is a combination of the conventional InC method with variable step size and bio-inspired dragonfly optimization (DFO) algorithms that can work efficiently in multiple weather conditions such as uniform irradiance and partial shading conditions. Meanwhile, the limitations associated with FLC, InC, and P&O algorithms were eliminated, with efficiency exceeding 97% using the improved hybrid algorithm-based MPPT method presented in [19].

In addition to the above discussed techniques, numerous extensions to and developments of the existing methods and novel methods are noticeable in the literature. Hussain Shareef et al. [9] propose a random forest-based approach to improve the MPPT performance, and it was tested under actual environmental conditions for 24 days to validate the accuracy and dynamic response. In addition to that, extreme seeking control (ESC) [20], an improved team game optimization algorithm [21], a fusion firefly algorithm [22], a hierarchical pigeon-inspired optimization-based method [23], a novel spline-MPPT technique [24], and an improved earthquake optimization algorithm [25] are some modern concepts used in tracking the maximum power point while addressing the different issues associated with it.

When considering the state-of-the-art methods, the integration of AI seems to be crucial to guarantee the tracking of GMPP while increasing the overall efficiency and performance of MPPT. Since the ANN portrays a medium algorithm complexity [26], less cost, and greater flexibility than other improved AI-based methods, it has played a major role in manifold hybrid methods. The neural network P&O controller is one of the most popular hybrid methods that combines ANN with the conventional P&O method [2]. In [27], the authors propose a unique approach to enhance the MPPT with the utilization of state estimation by sequential Monte-Carlo (SMC) filtering, which is assisted by the prediction of MPP via an ANN.

In most cases, the major shortcomings in MPPT occur in PS and rapidly changing weather conditions. Irradiance fluctuations that are limited to a short period lead the controller to change its state rapidly, resulting in unnecessary oscillations without converging to the MPP. Therefore, there is room for development in MPPT algorithms that are not affected by short-term fluctuations. If the future irradiance values are known, the controller can act accordingly in a smooth manner since the sudden irradiance fluctuations that are limited to a short time frame (which are called 'dummy peaks' in the irradiance pattern) [28] can be avoided and the change of direction of MPP can be aligned with the future trend. Moreover, it is important to note that, although the MPP primarily depends on solar irradiance, there is a considerable effect from the temperature variation as well. However, few articles in the literature have addressed this issue [29,30].

Despite the growing interest in AI and power electronics controllers for renewable energy systems, few studies have explored the potential hardware implementation of AI-based MPPT model for PV power optimization. These techniques generally require an expensive and advanced microprocessor to shorten computational time. Also, challenges arise in integrating AI-based MPPT tracking algorithms for existing control systems due to the lack of compatibility and reliable prediction of the optimal power point.

Taking into account all the above concerns, an ANN-based MPPT with the assistance of forecasted irradiance data is presented in this paper, which focuses on improving the efficiency and mitigating inefficient MPPT in varying environmental conditions. This hybrid method is a combination of an irradiance forecaster and a feedforward neural network (FNN), which strives to lessen the intermittent nature of solar energy to a considerable extent by predicting two future irradiance points and feeding them to the neural network along with present irradiance and temperature values. This eventually resulted in a more robust method, and depicted superior tracking performance and dynamic response when compared to other popular methods in the literature. The proposed method was validated via the MATLAB/Simulink environment using step responses and real irradiance data of different geographical conditions. Furthermore, the hardware implementation of the proposed method was demonstrated in a laboratory setup.

The key contributions of this paper are three-fold, as follows:

- The proposed hybrid MPPT algorithm that utilizes the existing FNN-based MPPT technique with the aid of an irradiance forecaster to lessen the effect of the intermittent nature of solar energy.
- The validation and comparison of the proposed method using MATLAB/Simulink using real irradiance data.
- The hardware implementation of the newly designed MPPT method for a single-phase grid-connected PV system.

This paper is organized as follows: The next section provides an overview of the PV system used, along with insights into the proposed method, including the theoretical background and data generation. Section 3 presents the experiments conducted in this study, with the details of hardware implementation, followed by the results and discussion in Section 4, which includes various test cases. Finally, the main conclusions of the paper are summarized in Section 5.

2. Materials and Methods

2.1. Proposed MPPT Algorithm

The PV system combined with the proposed MPPT algorithm used in this study is shown in Figure 1. The PV system consists of a solar PV array, boost converter, inverter, and utility grid with controllers. A single-phase-grid connected inverter with a boost converter arrangement was used for this PV system. The proposed MPPT algorithm uses a long-short term memory (LSTM) unit to predict future irradiance values. LSTM is a special recurrent neural network (RNN) that has time-varying inputs and targets. The unique gated unit structure of the LSTM enables it to remember information for a longer period of time [31–34]. In this method, LSTM weights are randomly initialized and tuned using backpropagation to minimize the irradiance prediction error. An FNN is used to predict the MPP voltage. This selection is based on the fact that an FNN requires significantly less computational cost compared to convolutional and attention networks, thereby making the model more efficient and simpler to implement. The weights of the FNN are initialized randomly. They are tuned with the backpropagation based on the biased MPP voltage error.

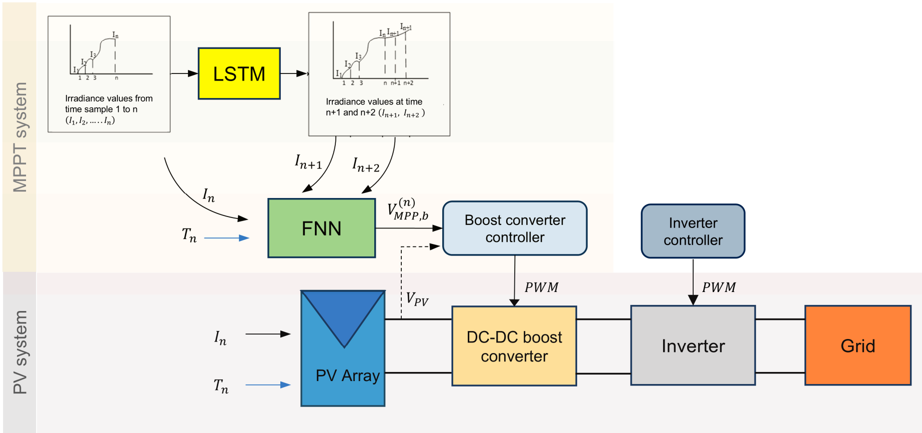

Figure 1. Proposed LSTM and FNN combined MPPT system.

Historical time series irradiance data from time 1 to time n are is fed to the LSTM unit, which predicts future irradiance values at time $n + 1$ and $n + 2$. The current irradiance value (I_n), along with the predicted irradiance values (I_{n+1} and I_{n+2}) and the temperature (T_n), are then used as inputs to the FNN. The FNN outputs the optimum MPP voltage ($V_{MPP,b}^{(n)}$), which is biased towards the possible upcoming MPP voltage values. This biased voltage helps the system to avoid responding to sudden fluctuations in solar irradiance. For example, Figure 2a shows an observed irradiance fluctuation from real irradiance data. In this figure, it can be seen that at point n, there is a sudden irradiance drop for a very short period. Due to this, existing MPPT algorithms change their MPP voltage according to the irradiance value at point n. At the next time step, irradiance increases, and the MPPT algorithm has to adjust the MPP voltage corresponding to the new irradiance value at points $n + 1$ as shown in Figure 2b. This may lead the controller to change its state rapidly where ultimately brief energy losses and transient instability may occur. With the proposed method, the effect of the sudden drop in the irradiance value at point n will be mitigated as the current MPP voltage is not only dependent on the irradiance value at point n, but also on future irradiance values at point $n + 1$ and $n + 2$. Then the controller tries to operate at the average MPP value at point b shown in Figure 2b. This helps to avoid unnecessary rapid fluctuations in MPP voltage, thus ensuring the smooth operation of the controller.

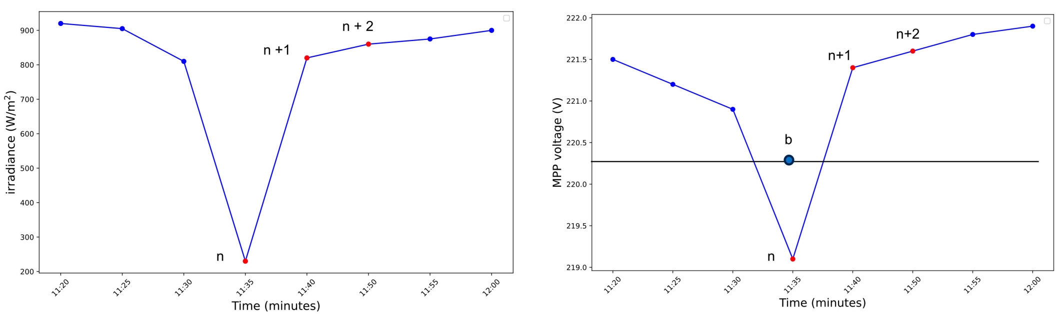

(**a**) (**b**)

Figure 2. (**a**) Observed irradiance fluctuation. (**b**) Corresponding MPP voltage for irradiance values.

The training process of the FNN is done using a dataset generated from Equation (1), which contains 1250 data points. When generating the dataset, the irradiance step size was selected as 25 W/m^2. Biased MPP voltage at time n ($V_{MPPb}^{(n)}$) is calculated by adding an ΔV value to the theoretical MPP voltage corresponding to the particular irradiance value at time n. This ΔV value is calculated using Equation (2), with the insight of the MPP voltages corresponding to the estimated future irradiance values.

$$V_{MPP,\ b}^{(n)} = V_{MPP}^{(n)} + \Delta V \tag{1}$$

where

$$\Delta V = \alpha \left[\frac{\left(v_{MPP}{}^{(n+1)} - v_{MPP}{}^{(n)} \right)}{v_{MPP}{}^{(n)}} \right] + \beta \left[\frac{\left(v_{MPP}{}^{(n+2)} - v_{MPP}{}^{(n+1)} \right)}{v_{MPP}{}^{(n+1)}} \right] \tag{2}$$

Here, $V_{mpp}^{(n)}$, $V_{mpp}^{(n+1)}$, and $V_{mpp}^{(n+2)}$ denote the MPP voltages that correspond to I_n, I_{n+1}, and I_{n+2} irradiances. α and β are the hyperparameters related to generating the training dataset of FNN. The selected α and β values are those that correspond to the dataset that is used to train the FNN that gives the maximum power. To select optimal α and β, the simulation was repeated multiple times with different values of α and β. The power output of the system for α = 1 and 1 < β < 15 for an irradiance step less than or equal to 25 W/m^2 is shown in Figure 3a. Similarly, the output power for β = 10 and 0.5 < α < 2 is shown in Figure 3b. In these figures, the *y*-axis refers to the captured power as a percentage of theoretical power. For clarity and to enhance the readability of the results, we have presented the power values in the figure for a single set of α and β values. A similar procedure was adopted to select the values for irradiance changes above 25 W/m^2. The rule base for selecting α and β is shown in Table 1.

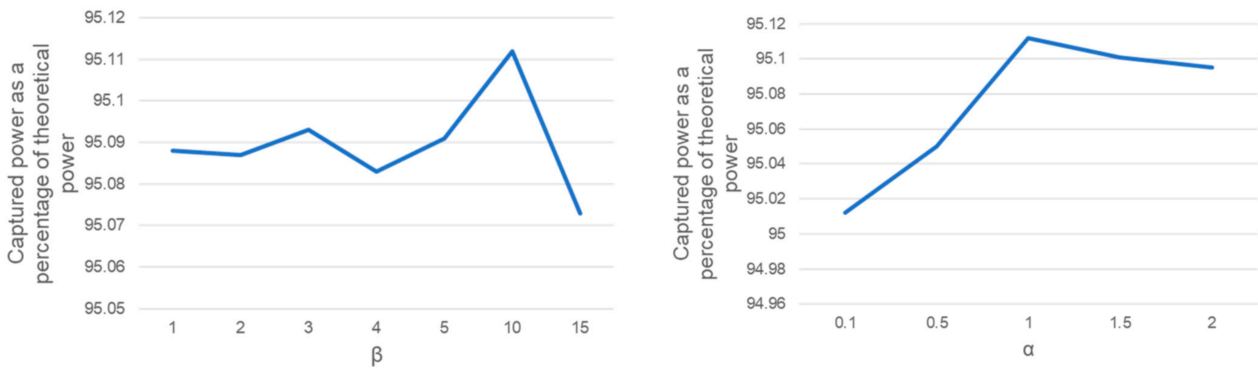

(**a**) (**b**)

Figure 3. Captured power as a percentage of theoretical power (a) when α = 1 and varying β; (b) when β = 10 and varying α.

Table 1. Rule base for selecting α and β.

Case	α	β
$I_n = I_{n+1} = I_{n+2}$	1	10
$\mid I_n - I_{n+1} \mid = 25$ W/m^2 & $\mid I_{n+1} - I_{n+2} \mid = 25$ W/m^2	1	10
$\mid I_n - I_{n+1} \mid > 25$ W/m^2 & $\mid I_{n+1} - I_{n+2} \mid > 25$ W/m^2	15	2

The trained FNN gives the biased MPP voltage and it is compared with the PV module voltage (V_{PV}). In the boost converter controller, the error signal is fed to the PI controller, which generates the duty ratio required to drive the PV voltage to the biased MPP voltage. This duty ratio is fed to the boost converter as a PWM gate signal.

The performance of the MPPT algorithms was assessed based on static and dynamic parameters. Static parameters evaluate the accuracy of the algorithm and the dynamic parameters evaluate the response speed of the particular algorithm.

2.2. Static Parameter

The theoretically available power at time n ($P_{TH}^{(n)}$) of a PV module for an instantaneous irradiance at time n (I_n) is given by Equation (3).

$$P_{TH}^{(n)} = \frac{\mathrm{P_{max}}}{\mathrm{I_{max}}} \times I_n \tag{3}$$

where $\mathrm{P_{max}}$ is the maximum power of the PV panel and $\mathrm{I_{max}}$ is the corresponding irradiance level at $\mathrm{P_{max}}$.

The power extracted from the PV module using the MPPT algorithm at time n ($P_{PV}^{(n)}$) is calculated from Equation (4).

$$P_{PV}^{(n)} = \mathrm{V_{PV}} \times \mathrm{I_{PV}} \tag{4}$$

where V_{PV} and I_{PV} denote the output voltage and current of the PV module.

Using Equations (3) and (4), instantaneous error at time n ($e^{(n)}$) is defined by Equation (5).

$$e^{(n)} = \mathrm{P_{TH}^{(n)}} - \mathrm{P_{PV}^{(n)}} \tag{5}$$

Two static parameters used to evaluate the performance of MPPT algorithms are defined using Equation (5).

1. Mean absolute error (MAE)

$$\mathrm{MAE} = \frac{\left|\sum_{\mathrm{i}=1}^{\mathrm{n}} \mathrm{e_i}\right|}{\mathrm{n}} \tag{6}$$

2. Mean squared error (MSE)

$$\mathrm{MSE} = \frac{\sum_{\mathrm{i}}^{\mathrm{n}} \mathrm{e_i^2}}{\mathrm{n}} \tag{7}$$

As the third static parameter, the total energy captured for a particular time period is used as defined in Equation (8).

3. Total energy captured (Total)

$$\mathrm{E_{total}} = \int_1^{\mathrm{t}} P_{PV} \mathrm{dt} \tag{8}$$

where P_{PV} is the captured power variation of the PV module.

2.3. Dynamic Parameters

To evaluate the response speeds of the algorithms, the rise time and the settling time were used [35]. Based on the PV power output in a step irradiance pattern, as shown in Figure 4, rise time and settling time were evaluated.

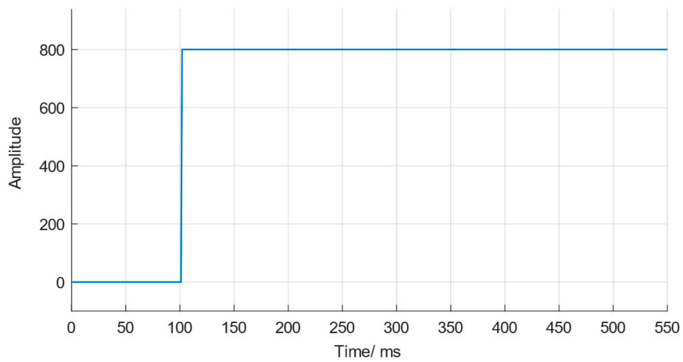

Figure 4. Step irradiance pattern to calculate rise time and settling time.

3. Experiments

In this study, various test cases were initiated using real irradiance data collected from different geographical regions in Sri Lanka. In terms of simulations, the MPPT algorithms were developed in the MATLAB/Simulink (version 2018b) simulation environment and executed on a processor with an Intel Core i7-7700HQ and 32 GB RAM running at 3.4 GHz.

3.1. Optimization of P&O MPPT Algorithm

The P&O algorithm is the most widely used MPPT algorithm in applications. Due to the widespread usage and competitive performance of the P&O algorithm, it is used as the base algorithm for the comparison. The fundamental principle of this method is the deliberate increment or decrement of voltage, after which the power is calculated and compared with the previous adjacent power value [36]. The performance of this method is highly dependent on the step size of the voltage perturbation. Therefore, it is important to optimize the step size to harvest the maximum possible power from the P&O method.

To obtain the optimum step size, the P&O algorithm was executed for a varying irradiance pattern that was developed using the real irradiance data collected in Kandy, Sri Lanka on a rainy day. The irradiance pattern is shown in Figure 5a. The five different step sizes given in Table 2 were used as Test Case A.

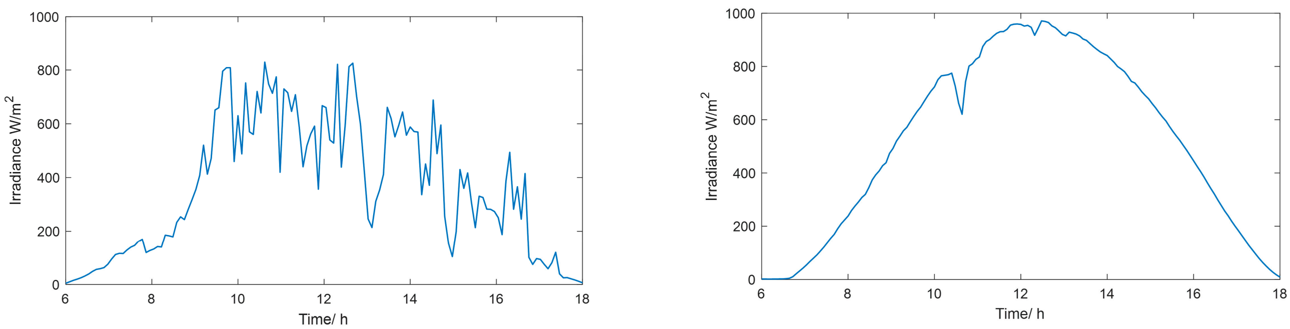

(**a**) (**b**)

Figure 5. (**a**) Volatile irradiance variation (Kandy on a rainy day); (**b**) smooth irradiance variation (Jaffna on a sunny day).

Table 2. Test case and scenario summary.

(A) P&O Performance Optimization for Different Step Sizes	(B) MPPT Performance for a Single Day	(C) Time Series Analysis of MPPT Methods for One Week	(D) Partial Shading Condition
(A.1) [1] Step size 0.5	(B.1) [2] P&O	(C.1) [3] P&O	(D.1) [4] P&O
(A.2) Step size 0.1	(B.2) INC	(C.2) ANN	(D.2) Proposed MPPT
(A.3) Step size 0.05	(B.3) Fuzzy	(C.3) Proposed MPPT	
(A.4) Step size 0.01	(B.4) PSO		
(A.5) Step size 0.005	(B.5) ANN		
	(B.6) Proposed MPPT		

[1] A.1—Scenario 1 in Test Case (A), [2] B.1—Scenario 1 in Test Case (B), [3] C.1—Scenario 1 in Test Case (C), and [4] D.1—Scenario 1 in Test Case (D).

3.2. Performance of Different MPPT Algorithms Under Single Day Irradiance Pattern

In this test case, different MPPT algorithms listed in Table 2 Case (B) were executed for two irradiance patterns. These two patterns are shown in Figure 5. The pattern with rapid changes was obtained in Kandy on a rainy day, while the smooth irradiance pattern was obtained in Jaffna on a sunny day. These are two representative geographical locations in Sri Lanka. The observation period was from 6.00 a.m. to 6.00 p.m. in this experiment.

3.3. Performance of MPPT Algorithm Under Irradiance Variation of One Week

The selected MPPT algorithms listed in Table 2 Case (C) were executed for combined irradiance patterns of seven days, which is a collection of smooth and fluctuating irradiance variations between 6.00 am and 6.00 pm every day, as shown in Figure 6.

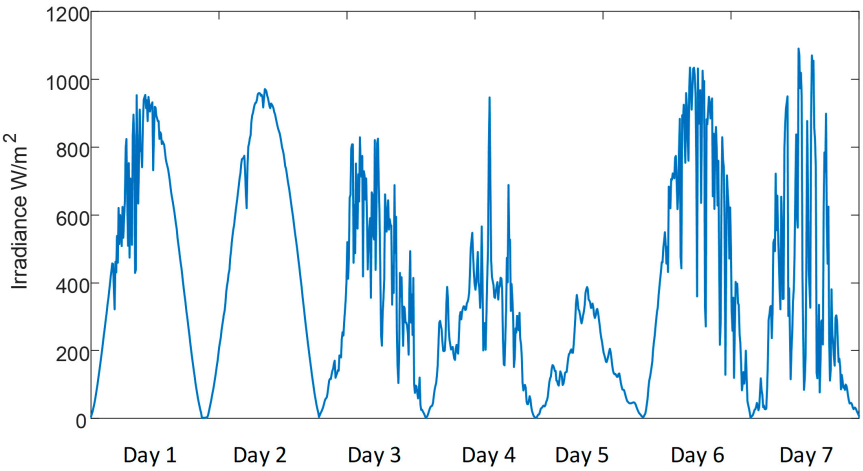

Figure 6. Irradiance variation of one week for the time series of MPPT performance.

3.4. Partial Shading Condition

In this test case, a PV array comprising six PV modules connected in series was utilized. To evaluate the performance of MPPT algorithms, as outlined in Table 2 Case (D), four distinct partial shading conditions were simulated. Partial shading conditions were achieved by assigning different irradiance levels to each PV module, as depicted in Figure 7.

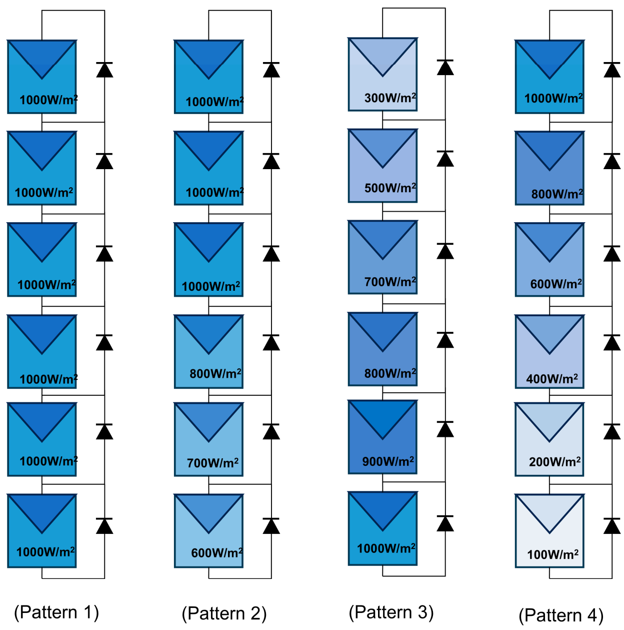

Figure 7. Arrangement of PV array under uniform and partial shading conditions.

3.5. Hardware Implementation of the Proposed MPPT Model

An experimental PV system was developed in the laboratory to validate the proposed MPPT algorithm, as shown in Figure 8. The generated power is fed to the local distribution network at University of Peradeniya. As our primary focus is on enhancing the active power generation of a PV system through the MPPT algorithm, we assumed that the network is equivalent to an infinite bus and that grid harmonics have no impact on the controller's operation. The boost converter controller was implemented using a floating-point digital signal processor (DSP) unit TMS320F28379D. In Figure 9, the trained model of the proposed MPPT algorithm was deployed on an ESP32 microcontroller, a system-on-chip (SoC) and embedded device suitable for AI model deployment. Though the training phase of our MPPT algorithm needs comparatively high computational power, for the deployment we used the pre-trained model, which requires less computational power, making it compatible with a simple embedded microcontroller. The current irradiance I_n and temperature T_n were measured by irradiance and temperature sensors, and these data were fed into the trained model installed on the ESP32 to predict optimal MPP voltage. The predicted optimal MPP voltage was then transmitted to the boost converter controller via a Serial Peripheral Interface (SPI) communication link to regulate its operation.

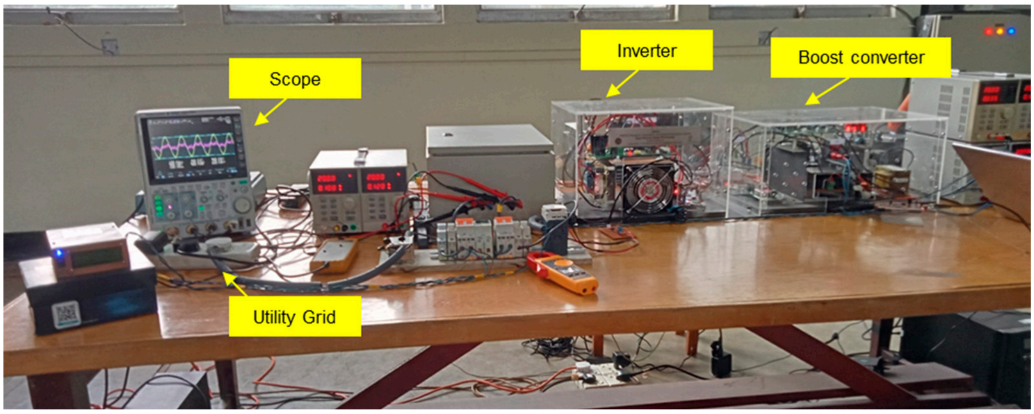

Figure 8. Experimental setup of PV system.

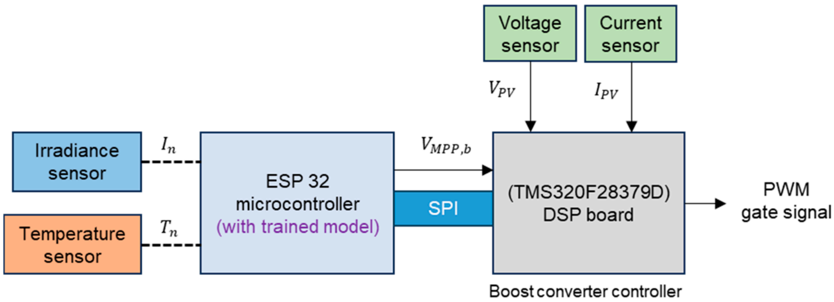

Figure 9. Sensor and controller arrangement of DC-DC boost converter.

4. Results and Discussion

This section highlights the performance of the proposed MPPT algorithms under different irradiance variations. First, the results for Test Case (A) are analyzed, focusing on both static and dynamic parameters. Next, the power captured by the grid in the simulation models of all algorithms is evaluated for two different irradiance patterns: one with volatile variations and the other with smooth variations. Following this, a time series analysis is conducted for the best-performing algorithms using single-day simulations. Further, the performance of the MPPT algorithms is assessed under partial shading conditions.

4.1. Optimizing P&O MPPT Performance

The simulation model was developed using six series-connected Yingli YL 300P-35b [37] PV modules. The voltage perturbation step size of the P&O MPPT algorithm was adjusted according to the scenarios outlined in Table 2. The results, including MSE, MAE, and total energy captured, were calculated for the irradiance pattern depicted in Figure 5a. Additionally, the rise time and settling time, determined by applying the step input shown in Figure 4, were obtained and are presented in Table 3. The output power variation along with the dynamic responses is illustrated in Figure 10.

Table 3. P&O MPPT method performance comparison for different voltage perturbation step sizes.

Scenario	MAE	MSE	E (kWh)	Rise Time (ms)	Settling Time (ms)
(A.1) step size 0.5	990.50	25.06	6.50	13.15	27.86
(A.2) step size 0.1	710.04	23.45	6.70	37.02	47.00
(A.3) step size 0.05	682.50	20.80	7.10	65.09	84.00
(A.4) step size 0.01	680.48	19.64	7.15	10.30	320.00
(A.5) step size 0.005	682.76	19.11	7.09	10.00	542.60

MAE—mean absolute error, MSE—mean squared error, E—total energy captured.

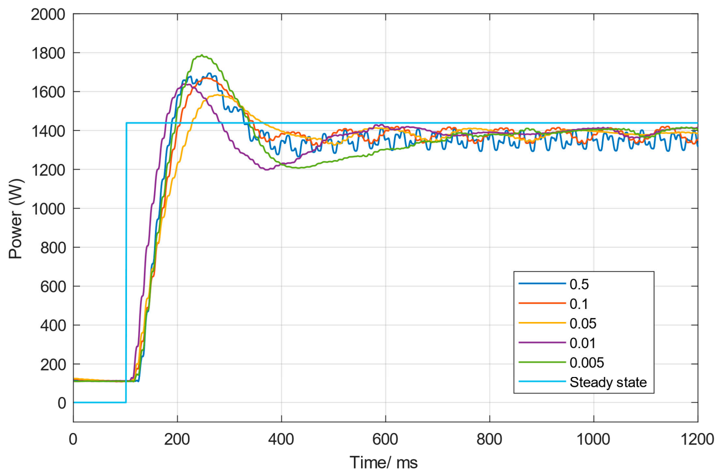

Figure 10. Dynamic response analysis of P&O method at different step sizes.

It can be observed that a step size of 0.05 (A.3) provides a good balance, achieving a low MAE (682.50) and MSE (20.80), while also capturing higher total energy (7.10 kWh). Its rise time (65.09 ms) and settling time (84 ms) are also moderate, suggesting that it maintains a compromise between fast convergence and steady-state accuracy. Therefore, a step size of 0.05 was selected for further comparison with the proposed method.

4.2. MPPT Performance for a Single Day (Test Case B)

The irradiance patterns shown in Figure 4 were used as inputs to the simulation model. The ideal power captured, calculated using Equation (3), was compared to the actual power captured by the simulated model under various MPPT algorithms. The MAE, MSE, and total energy captured were calculated using Equations (6)–(8), respectively, and are summarized in Table 4. For a day having volatile irradiance, the ideal available energy was 7.3538 kWh, while for a smooth irradiance day, it was 11.888 kWh. It can be observed that the proposed MPPT method captured the highest energy under both volatile and smooth irradiance conditions. Additionally, the proposed novel ANN-based MPPT method demonstrated the lowest MAE and MSE values, indicating superior accuracy compared to other methods. In contrast, MPPT algorithms based on fuzzy logic and PSO captured the least amount of energy and exhibited higher MAE and MSE values. Figure 11 illustrates the comparison between the theoretical and observed power under the irradiance pattern shown in Figure 5a or both the proposed MPPT method and the optimized P&O method. It also shows the MPP voltage variations for these two methods.

To analyze the dynamic performance of MPPT algorithms, a step irradiance input as shown in Figure 4 was fed to the algorithm and the response was analyzed considering the rise time and settling time. Table 5 shows the results of all the responses for various MPPT algorithms.

Table 4. MPPT method performance comparison in different irradiance variations.

	Kandy Rainy Day			Jaffna Sunny Day		
Scenario	**MSE**	**MAE**	**E**	**MSE**	**MAE**	**E**
(B.1) P&O	682.50	20.80	7.10	249.09	10.72	11.53
(B.2) INC	674.94	23.45	7.02	365.04	10.07	11.37
(B.3) Fuzzy	2413.00	33.52	6.79	1236.30	19.68	11.10
(B.4) PSO	1478.90	33.89	6.98	1250.40	22.84	10.95
(B.5) ANN	661.30	20.67	7.14	145.50	9.56	11.69
(B.6) proposed MPPT	612.42	18.86	7.23	110.20	9.21	11.79

MAE—mean absolute error, MSE—mean squared error, E—total energy captured.

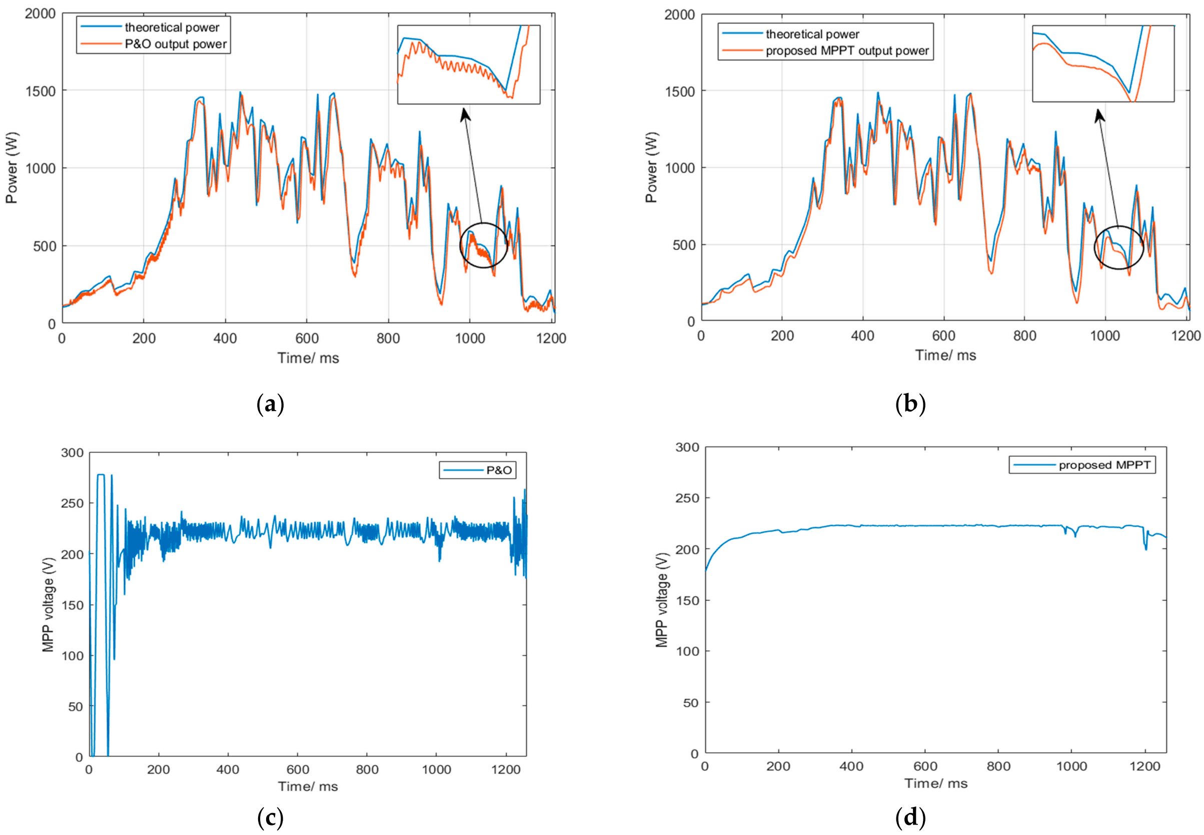

Figure 11. (**a**) Generated power variation with input power of P&O method; (**b**) generated power variation with input power of proposed MPPT method; (**c**) MPP voltage variation of P&O method; (**d**) MPP voltage variation of proposed MPPT method.

Table 5. Dynamic response results summary.

Scenario	Rise Time (ms)	Settling Time (ms)
(B.1) P&O	16.90	24
(B.2) INC	787.90	217
(B.3) Fuzzy	19.70	42
(B.4) PSO	6.40	39
(B.5) ANN	70.90	224
(B.6) proposed MPPT	4.68	19

4.3. MPPT Performance for One Week Simulation

To assess the long-term performance of the best-performing MPPT algorithms, the irradiance variation shown in Figure 5 was used to evaluate their effectiveness. Table 6 summarizes the MSE, MAE, and total energy captured by each MPPT algorithm over the specified period. The theoretical total energy available during this time was calculated to be 57.236 kWh. Based on the data in Table 5, it can be concluded that the proposed MPPT algorithm outperformed the others. Specifically, the proposed method demonstrated a 3% improvement in energy-capturing capability compared to the traditional P&O MPPT algorithm.

Table 6. Results summary of one-week simulation.

Scenario	Mean Squared Error (MSE)	Mean Absolute Error (MAE)	Total Energy Captured (kWh)	% of Energy Captured w.r.t the Theoretically Available Energy
(C.1) P&O	738.26	20.27	54.40	95.04%
(C.2) ANN	734.37	19.67	55.44	96.86%
(C.3) proposed MPPT	727.66	18.54	56.14	98.08%

4.4. Under Partial Shading Conditions

Figure 12 illustrates the output power variation of two different MPPT algorithms P&O and the proposed MPPT algorithm under four different partial shading patterns. The proposed MPPT method proves to be more effective in handling partial shading scenarios, offering better performance in terms of stability and accurate power tracking, which leads to higher energy efficiency.

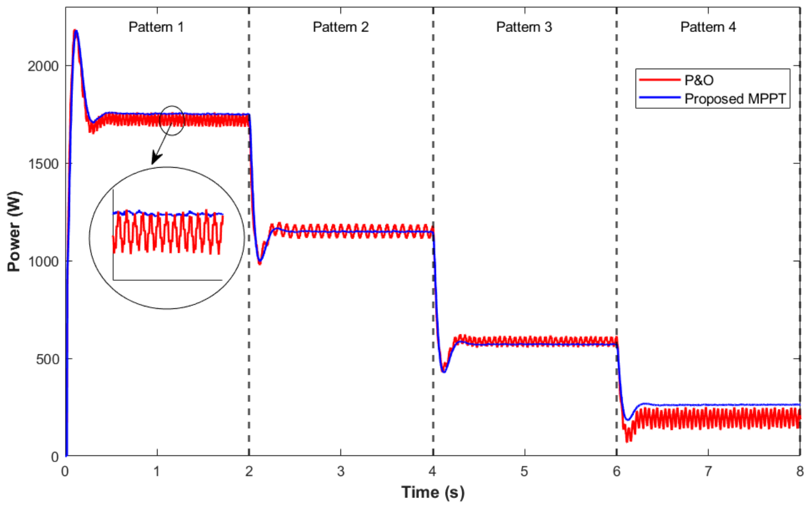

Figure 12. Power variation of P&O and proposed MPPT method under partial shading condition.

4.5. Hardware Implementation

Three series-connected solar panels with the electrical properties described in Table 7 are used in the PV array. Figure 13 illustrates the measured data, namely irradiance, MPP voltage, and power fed to the grid.

Table 7. PV panel electrical characteristics.

Item	Value
Solar panel	YL330P-25b 1500 V
Power rating	330 W
Number of cells	72
MPPT voltage (V_{MPP})	37.4 V
Open circuit voltage (V_{OC})	46.4 V
Short circuit current (I_{SC})	9.29 A

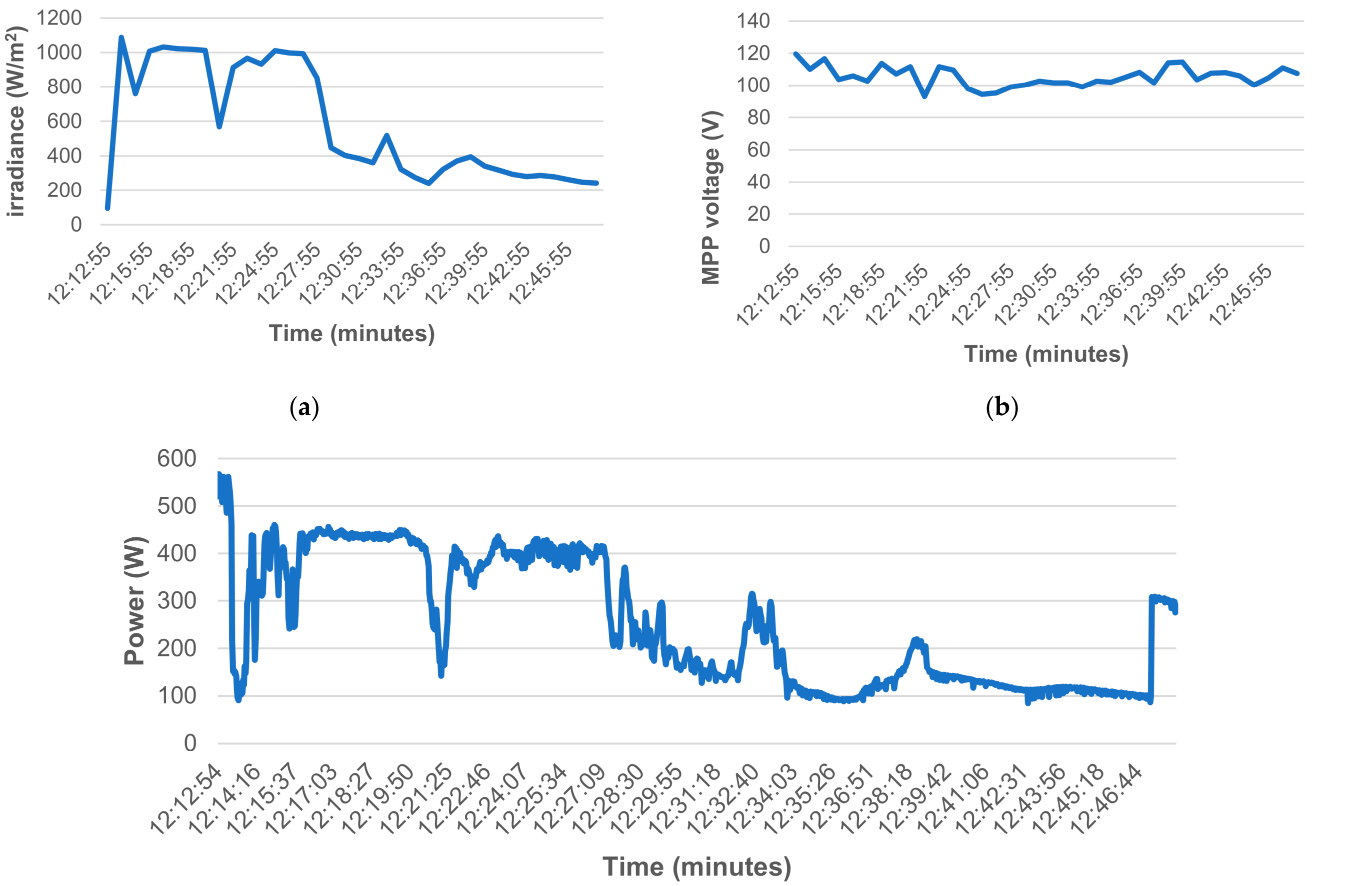

(**a**) (**b**) (**c**)

Figure 13. (**a**) Measured Irradiance data; (**b**) measured MPP voltage data; (**c**) measured power data.

5. Conclusions

This study presents a novel maximum power point tracking (MPPT) method that integrates LSTM networks for irradiance prediction with an FNN to enhance efficiency and stabilize power output. The proposed algorithm consistently outperformed existing methods, demonstrating superior performance in terms of MSE and MAE when compared to theoretical energy capture. It achieved notable improvements in energy-capturing efficiency, reduced fluctuations around the maximum power point, and excelled under partial shading conditions. When benchmarked against five state-of-the-art MPPT algorithms, the proposed method showed superior tracking accuracy and captured 3% more energy compared to the conventional Perturb and Observe (P&O) algorithm, all while maintaining a lower computational cost. This energy gain is expected to scale significantly over prolonged operation, highlighting the algorithm's long-term advantages. Additionally, the method achieved shorter rise and settling times with minimal oscillations around the MPP, ensuring a faster and more stable response. In terms of practical implementation, the proposed approach can be seamlessly deployed using a pre-trained model, which reduces computational demands during real-time operation. Its successful integration on a commercially available DSP board underscores its adaptability for use with PV inverters of varying scales. Overall, the proposed MPPT method demonstrated advancements in both energy capture and operational efficiency, making it a robust solution for enhancing solar panel performance. This work also establishes a foundational framework for incorporating AI-driven technologies into power electronics, paving the way for further exploration of AI's potential in optimizing solar inverter performance and advancing renewable energy systems.

Author Contributions: Conceptualization, A.B., K.R., R.D. and H.U.; methodology, A.B., K.R., R.D. and J.E.; software, A.B. and R.D.; validation, A.B., K.R. and R.D.; formal analysis, A.B., K.R. and J.E.; investigation, J.E. and R.G.; resources, A.B. and K.R.; data curation, A.B., K.R. and R.D.; writing—original draft preparation, A.B. and K.R.; writing—review and editing, J.E. and R.G.; visualization, A.B. and K.R.; supervision, J.E., P.E. and R.G.; project administration, J.E. and P.E. All authors have read and agreed to the published version of the manuscript.

Funding: This research received funding from the Multidisciplinary AI Research Centre of the University of Peradeniya.

Data Availability Statement: Data are contained within the article.

Conflicts of Interest: The authors declare no conflicts of interest.

References

1. Lee, H.S.; Yun, J.J. Advanced MPPT Algorithm for Distributed Photovoltaic Systems. *Energies* **2019**, *12*, 3576. [CrossRef]
2. Yap, K.Y.; Sarimuthu, C.R.; Lim, J.M.Y. Artificial Intelligence Based MPPT Techniques for Solar Power System: A review. *J. Mod. Power Syst. Clean Energy* **2020**, *8*, 1043–1059.
3. Guerra, M.I.S.; Ugulino De Araújo, F.M.; Dhimish, M.; Vieira, R.G. Assessing Maximum Power Point Tracking Intelligent Techniques on a PV System with a Buck–Boost Converter. *Energies* **2021**, *14*, 7453. [CrossRef]
4. Baba, A.O.; Liu, G.; Chen, X. Classification and Evaluation Review of Maximum Power Point Tracking Methods. *Sustain. Futures* **2020**, *2*, 100020. [CrossRef]
5. Khanam, J.J.; Foo, S.Y. Modeling of a Photovoltaic Array in MATLAB Simulink and Maximum Power Point Tracking Using Neural Network. *J. Electr. Electron. Syst.* **2018**, *7*, 3. Available online: https://www.omicsonline.org/open-access/modeling-of-a-photovoltaic-array-in-matlab-simulink-and-maximum-power-point-tracking-using-neural-network-2332-0796-1000263-104991.html (accessed on 3 November 2024). [CrossRef]
6. Hlaili, M.; Mechergui, H. Comparison of Different MPPT Algorithms with a Proposed One Using a Power Estimator for Grid Connected PV Systems. *Int. J. Photoenergy* **2016**, *2016*, 1728398. [CrossRef]
7. Tajuddin, M.F.N.; Arif, M.S.; Ayob, S.M.; Salam, Z. Perturbative methods for maximum power point tracking (MPPT) of photovoltaic (PV) systems: A review: Perturbative methods for MPPT. *Int. J. Energy Res.* **2015**, *39*, 1153–1178. [CrossRef]
8. Villegas-Mier, C.G.; Rodriguez-Resendiz, J.; Álvarez-Alvarado, J.M.; Rodriguez-Resendiz, H.; Herrera-Navarro, A.M.; Rodríguez-Abreo, O. Artificial Neural Networks in MPPT Algorithms for Optimization of Photovoltaic Power Systems: A Review. *Micromachines* **2021**, *12*, 1260. [CrossRef]
9. Shareef, H.; Mutlag, A.H.; Mohamed, A. Random Forest-Based Approach for Maximum Power Point Tracking of Photovoltaic Systems Operating under Actual Environmental Conditions. *Comput. Intell. Neurosci.* **2017**, *2017*, 1673864. [CrossRef]
10. Mohamed, S.A.; Abd El Sattar, M. A comparative study of P&O and INC maximum power point tracking techniques for grid-connected PV systems. *SN Appl. Sci.* **2019**, *1*, 174.
11. Murtaza, A.F.; Sher, H.A.; Spertino, F.; Ciocia, A.; Noman, A.M.; Al-Shamma'a, A.A.; Alkuhayli, A. A Novel MPPT Technique Based on Mutual Coordination between Two PV Modules/Arrays. *Energies* **2021**, *14*, 6996. [CrossRef]
12. Xu, L.; Cheng, R.; Yang, J. A New MPPT Technique for Fast and Efficient Tracking under Fast Varying Solar Irradiation and Load Resistance. *Int. J. Photoenergy* **2020**, *2020*, 6535372. [CrossRef]
13. Windarko, N.A.; Nizar Habibi, M.; Sumantri, B.; Prasetyono, E.; Efendi Moh, Z.; Taufik. A New MPPT Algorithm for Photovoltaic Power Generation under Uniform and Partial Shading Conditions. *Energies* **2021**, *14*, 483. [CrossRef]
14. Merchaoui, M.; Hamouda, M.; Sakly, A.; Mimouni, M.F. Fuzzy logic adaptive particle swarm optimisation based MPPT controller for photovoltaic systems. *IET Renew. Power Gener.* **2020**, *14*, 2933–2945. [CrossRef]
15. Imtiaz, T.; Khan, B.H.; Khanam, N. Fast and improved PSO (FIPSO)-based deterministic and adaptive MPPT technique under partial shading conditions. *IET Renew. Power Gener.* **2020**, *14*, 3164–3171. [CrossRef]
16. Joisher, M.; Singh, D.; Taheri, S.; Espinoza-Trejo, D.R.; Pouresmaeil, E.; Taheri, H. A Hybrid Evolutionary-Based MPPT for Photovoltaic Systems Under Partial Shading Conditions. *IEEE Access* **2020**, *8*, 38481–38492. [CrossRef]
17. Norouzzadeh, E.; Ale Ahmad, A.; Saeedian, M.; Eini, G.; Pouresmaeil, E. Design and Implementation of a New Algorithm for Enhancing MPPT Performance in Solar Cells. *Energies* **2019**, *12*, 519. [CrossRef]
18. Sarwar, S.; Javed, M.Y.; Jaffery, M.H.; Arshad, J.; Rehman, A.U.; Shafiq, M.; Choi, J.-G. A Novel Hybrid MPPT Technique to Maximize Power Harvesting from PV System under Partial and Complex Partial Shading. *Appl. Sci.* **2022**, *12*, 587. [CrossRef]
19. Bataineh, K. Improved hybrid algorithms-based MPPT algorithm for PV system operating under severe weather conditions. *IET Power Electron.* **2019**, *12*, 703–711. [CrossRef]
20. Tchouani Njomo, A.F.; Kenne, G.; Douanla, R.M.; Sonfack, L.L. A Modified ESC Algorithm for MPPT Applied to a Photovoltaic System under Varying Environmental Conditions. *Int. J. Photoenergy* **2020**, *2020*, 1956410. [CrossRef]
21. Shams, I.; Mekhilef, S.; Tey, K.S. Improved-Team-Game-Optimization-Algorithm-Based Solar MPPT With Fast Convergence Speed and Fast Response to Load Variations. *IEEE Trans. Ind. Electron.* **2021**, *68*, 7093–7103. [CrossRef]

22. Huang, Y.P.; Huang, M.Y.; Ye, C.E. A Fusion Firefly Algorithm with Simplified Propagation for Photovoltaic MPPT Under Partial Shading Conditions. *IEEE Trans. Sustain. Energy* **2020**, *11*, 2641–2652. [CrossRef]
23. Zhao, Z.; Zhang, M.; Zhang, Z.; Wang, Y.; Cheng, R.; Guo, J.; Yang, P.; Lai, C.S.; Li, P.; Lai, L.L. Hierarchical Pigeon-Inspired Optimization-Based MPPT Method for Photovoltaic Systems Under Complex Partial Shading Conditions. *IEEE Trans. Ind. Electron.* **2022**, *69*, 10129–10143. [CrossRef]
24. Ostadrahimi, A.; Mahmoud, Y. Novel Spline-MPPT Technique for Photovoltaic Systems Under Uniform Irradiance and Partial Shading Conditions. *IEEE Trans. Sustain. Energy* **2021**, *12*, 524–532. [CrossRef]
25. Mendez, E.; Ortiz, A.; Ponce, P.; Macias, I.; Balderas, D.; Molina, A. Improved MPPT Algorithm for Photovoltaic Systems Based on the Earthquake Optimization Algorithm. *Energies* **2020**, *13*, 3047. [CrossRef]
26. Zečević, Ž.; Rolevski, M. Neural Network Approach to MPPT Control and Irradiance Estimation. *Appl. Sci.* **2020**, *10*, 5051. [CrossRef]
27. Chen, L.; Wang, X. Enhanced MPPT method based on ANN-assisted sequential Monte–Carlo and quickest change detection. *IET Smart Grid* **2019**, *2*, 635–644. [CrossRef]
28. Sai, B.S.V.; Khadtare, S.A.; Chatterjee, D. A dummy peak elimination based MPPT technique for PV generation under partial shading condition. *IET Renew. Power Gener.* **2021**, *15*, 2438–2451. [CrossRef]
29. Vicente, E.M.; Santos Vicente, P.; Moreno, R.L.; Ribeiro, E.R. High-efficiency MPPT method based on irradiance and temperature measurements. *IET Renew. Power Gener.* **2020**, *14*, 986–995. [CrossRef]
30. Chellakhi, A.; El Beid, S.; Abouelmahjoub, Y. An Improved Maximum Power Point Approach for Temperature Variation in PV System Applications. *Int. J. Photoenergy* **2021**, *2021*, 9973204. [CrossRef]
31. Siami-Namini, S.; Tavakoli, N.; Namin, A.S. The Performance of LSTM and BiLSTM in Forecasting Time Series. In Proceedings of the 2019 IEEE International Conference on Big Data (Big Data), Los Angeles, CA, USA, 9–12 December 2019; IEEE: Piscataway, NJ, USA, 2019; pp. 3285–3292. Available online: https://ieeexplore.ieee.org/document/9005997/ (accessed on 3 November 2024).
32. Yufang, L.; Mingnuo, C.; Wanzhong, Z. Investigating long-term vehicle speed prediction based on BP-LSTM algorithms. *IET Intell. Transp. Syst.* **2019**, *13*, 1281–1290. [CrossRef]
33. Liu, R.; Wei, J.; Sun, G.; Muyeen, S.M.; Lin, S.; Li, F. A short-term probabilistic photovoltaic power prediction method based on feature selection and improved LSTM neural network. *Electr. Power Syst. Res.* **2022**, *210*, 108069. [CrossRef]
34. Zhao, H.; Zhao, Z.; Wang, H.; Yue, Y. Short-term Photovoltaic Power Prediction based on DE-GWO-LSTM. In Proceedings of the 2020 IEEE International Conference on Mechatronics and Automation (ICMA), Beijing, China, 2–5 August 2020; IEEE: Piscataway, NJ, USA, 2020; pp. 1681–1686. Available online: https://ieeexplore.ieee.org/document/9233555/ (accessed on 10 April 2024).
35. ECE 486 Control Systems [Internet]. Available online: https://courses.grainger.illinois.edu/ece486/fa2018/handbook/lec06.html (accessed on 3 November 2024).
36. Swaminathan, N.; Lakshminarasamma, N.; Cao, Y. A Fixed Zone Perturb and Observe MPPT Technique for a Standalone Distributed PV System. *IEEE J. Emerg. Sel. Top. Power Electron.* **2022**, *10*, 361–374. [CrossRef]
37. Yingli Solar YL300P-35B Installation and User Manual Pdf Download | ManualsLib [Internet]. Available online: https://www.manualslib.com/manual/1352582/Yingli-Solar-Yl300p-35b.html (accessed on 3 November 2024).